BBA - Molecular Basis of Disease 1863 (2017) 2202–2209

Contents lists available at ScienceDirect

BBA - Molecular Basis of Disease

journal homepage: www.elsevier.com/locate/bbadis

# Cell death induced by mitochondrial complex I inhibition is mediated by Iron Regulatory Protein 1

Pamela J. Urrutia, Pabla Aguirre, Victoria Tapia, Carlos M. Carrasco, Natalia P. Mena, Marco T. Núñez*

*Biology Department, Faculty of Sciences, Universidad de Chile, Santiago, Chile*

ARTICLE INFO

*Keywords:*
Mitochondrial dysfunction
IRP1
Iron accumulation
Oxidative damage
Ferritin

ABSTRACT

Mitochondrial dysfunction and oxidative damage, often accompanied by elevated intracellular iron levels, are pathophysiological features in a number of neurodegenerative processes. The question arises as to whether iron dyshomeostasis is a consequence of mitochondrial dysfunction. Here we have evaluated the role of Iron Regulatory Protein 1 (IRP1) in the death of SH-SY5Y dopaminergic neuroblastoma cells subjected to mitochondria complex I inhibition. We found that complex I inhibition was associated with increased levels of transferrin receptor 1 (TfR1) and iron uptake transporter divalent metal transporter 1 (DMT1), and decreased levels of iron efflux transporter Ferroportin 1 (FPN1), together with increased $^{55}$Fe uptake activity and an increased cytoplasmic labile iron pool. Complex I inhibition also resulted in increased oxidative modifications and increased cysteine oxidation that were inhibited by the iron chelators desferoxamine, M30 and Q1. Silencing of IRP1 abolished the rotenone-induced increase in $^{55}$Fe uptake activity and it protected cells from death induced by complex I inhibition. IRP1 knockdown cells presented higher ferritin levels, a lower iron labile pool, increased resistance to cysteine oxidation and decreased oxidative modifications. These results support the concept that IRP1 is an oxidative stress biosensor that mediates iron accumulation and cell death when deregulated by mitochondrial dysfunction. IRP1 activation, secondary to mitochondrial dysfunction, may underlie the events leading to iron dyshomeostasis and neuronal death observed in neurodegenerative disorders with an iron accumulation component.

## 1. Introduction

Cellular iron homeostasis is largely maintained by the binding of cytosolic iron regulatory proteins IRP1 and IRP2) to iron responsive elements (IREs) that are found in the untranslated regions of mRNAs that codify for the principal proteins of cellular iron homeostasis [1,2]. IRPs are activated under conditions of low cell iron, which results in increased iron uptake and diminished iron storage capacity [3,4]. The two known IRP isoforms, IRP1 and IRP2, share the same IRE binding activity but they are regulated by different mechanisms. IRP1 is a bifunctional protein containing a [4Fe-4S] iron-sulfur cluster prosthetic group. In its holo form, IRP1 is active as a cytosolic aconitase, whereas upon the loss of its iron-sulfur cluster it serves as an IRE binding protein [5,6]. In contrast, IRP2 is activated by hypoxia [7] and it is down-regulated by ubiquitination mediated by an iron-responsive E3 ubiquitin ligase-FBXL5 complex and proteasome degradation [3,8,9]. Both IRP1 and IRP2 knockout mice are viable, but the double knockout (*Irp1* −/− *Irp2* −/−) mice are embryonically lethal [10], indicating that IRPs play a crucial role in maintaining murine embryo's viability.

Iron dyshomeostasis, often coupled to mitochondrial dysfunction, plays an important role in the development of a number of neurodegenerative pathologies known as neurodegeneration with brain iron accumulation, characterized by the presence of high brain iron levels particularly within the basal ganglia [11–15]. The capacity of redox-active iron to generate free radicals underlies the “metal-based neurodegeneration hypothesis” [16]. According to this hypothesis, reactive oxygen species (ROS) that are generated by redox-active metals like iron and copper cause peroxidation of membrane phospholipids. This peroxidation leads to the formation of reactive aldehydes that react with proteins producing misfolded aggregates that overwhelm the

*Abbreviations:* 4-HNE, 4-hydroxy-2-nonenal; 6-OHDA, 6-hydroxydopamine; BSO, buthioninesulfoximine; DFO, Deferoxamine; DMT1, divalent metal transporter 1; ELISA, enzyme-linked immunosorbent assay; FPN1, Ferroportin 1; IRE, iron responsive element; IRP, iron regulatory protein; LDH, lactate dehydrogenase; M30, 5-(*N*-methyl-*N*-propargylaminomethyl)-8-hydroxyquinoline; MPTP, 1-methyl-4-phenyl-1,2,3,6-tetrahydropyridine; PD, Parkinson's disease; Q1, 5-((methylamino)methyl)-8-hydroxyquinoline; ROS, reactive oxygen species; TfR1, transferrin receptor 1

* Corresponding author at: Iron and Biology of Aging Laboratory, Faculty of Sciences, University of Chile, Las Palmeras 3425, Santiago 7800024, Chile.
*E-mail address:* mnunez@uchile.cl (M.T. Núñez).

http://dx.doi.org/10.1016/j.bbadis.2017.05.015
Received 22 November 2016; Received in revised form 18 April 2017; Accepted 10 May 2017
Available online 11 May 2017

ubiquitin/proteasome protein degradation system and accumulate within intracellular inclusion bodies [16].

A link between ROS and iron homeostasis was established with the observation that ROS spuriously activate IRP1 [17–19]. In addition to oxidative stress, IRP1 is activated by a decreased mitochondrial iron-sulfur cluster synthesis resulting from an inhibition of mitochondrial complex I [20,21]. Similarly, inhibition of complex I by toxins like MPTP, rotenone and aminochrome results in an iron-accumulation phenotype in animal and cell models of Parkinson's disease [22–24].

Based upon the observation that the inhibition of complex I results in decreased iron-sulfur cluster synthesis and IRP1 activation, in this work we tested the hypothesis that IRP1 is a redox sensor that when activated by complex I inhibition mediates iron accumulation, oxidative damage and cell death.

## 2. Material and methods

### 2.1. Cells

Human neuroblastoma SH-SY5Y cells (CRL-2266; American Type Culture Collection, Rockville, MD) were cultured in MEM/F12 medium supplemented with 10% fetal bovine serum and 5 mM glutamine as described [25].

### 2.2. Antibodies and iron chelators

Primary antibodies used were rabbit polyclonal anti-FPN1 (Alpha Diagnostics) and anti-TfR1 (Santa Cruz Biotechnology). Polyclonal rabbit anti-human ferritin and peroxidase-labeled rabbit anti-human ferritin antibodies were purchased from DAKO Corporation. Anti-pan DMT1 prepared against the amino-terminal sequence MVLGPEQK MSDDSVSGDH [26] was used at a dilution of 1:1000. Rabbit polyclonal anti-IRP2 antibody UT29 [3] was the kind gift of Dr. E. Liebold. Rabbit polyclonal anti-IRP1 antibody 2170, prepared against the IRP1 sequence VDFNRRADSLQKNQDLEFERNR [27], was the kind gift of Dr. R. Eisenstein. Anti-HNE antibody ab46545 was purchased from Abcam.

Iron chelators desferoxamine (DFO), 5-(*N*-methyl-*N*-propargylaminomethyl)-8-hydroxyquinoline (M30) and 2,2′-dipyridyl were purchased from Sigma-Aldrich. Iron chelator 5-((methylamino)methyl)-8-hydroxyquinoline (Q1) was synthesized as described [28].

### 2.3. Inhibition of complex I activity and detection of iron homeostasis proteins

The activity of complex I was inhibited by incubation for 24 h with varied concentrations of rotenone (1 to 5 μM) as described [20]. This concentration range falls well within the range of concentrations used in the literature [29–31]. Protein levels of TfR1, DMT1 and FPN1 were determined by Western blot as described [26]. Ferritin was determined by a sandwich ELISA as described [32].

### 2.4. Cytotoxicity assay

Cytotoxicity was assessed in 96-well microplates using a LDH release assay (Aras et al. 2008). LDH activity in the culture medium was expressed as percentage of the activity determined in the cell culture medium without treatment.

### 2.5. Cell extracts and RNA electrophoretic mobility shift assay (EMSA)

Cell extracts were prepared by a modification of a published method [19] optimized for the EMSA kit used in this study. Briefly, cells were detached from the culture dish by incubation for 15 min on ice with a buffer containing 40 mM Tris pH 7.5, 100 mM NaCl and 1 mM EDTA. Cells were sedimented by centrifugation and they were lysed with a lysis buffer: 50 μL per $1 \times 10^6$ cells of 10 mM Hepes, pH 7.5, 3 mM $MgCl_3$, 40 mM KCl, 1 mM phenylmethylsulfonyl fluoride, 1 mM dithiothreitol, 0.5% NP40 and a protease inhibitor cocktail (ROCHE). After incubation for 15 min on ice, the mixture was sedimented for 10 min at 10,000 × *g* and stored in aliquots at − 20 °C. The IRP binding activity was determined with a LightShift chemiluminescent RNA EMSA Kit (Thermo Scientific No. 20158). A modification of the manufacturer's protocol was introduced that allowed for the cleaning of non-specific bands. Briefly, 20 μg of protein extract in the 10 mM Hepes buffer described above was incubated for 30 min at room temperature with 1.2 ng of biotin-labeled IRE (UCCUGCUUCAACAGUGCUUGGACGGAA C-biotin) (BioSynthesis Inc.). The mixture was loaded into an 8% non-denaturating polyacrylamide gel (Mini-PROTEAN, Bio-Rad Inc.) and the proteins were resolved for 1.5 h at 100 V. IRP-IRE binding activity was developed with Streptavidin-Horseradish Peroxidase Conjugate (Thermo Fisher Scientific) as instructed by the manufacturer.

### 2.6. Determination of the cytoplasmic labile iron pool

Iron levels in the cytoplasmic labile iron pool were estimated by a calcein dequenching assay (Calcein-AM Invitrogen-Molecular Probes) as described [28,33]. Briefly, calcein decreases its fluorescence when bound to iron. The increase in fluorescence in calcein-loaded cells upon addition of the iron chelator 2,2′-dipyridyl is directly proportional to the cytoplasmic labile iron pool.

### 2.7. IRP1 knockdown in SH-SY5Y neuroblastoma cells

ShRNA against human IRP1 (gene name: *ACO1*) was obtained from the RNAi Consortium, distributed by Sigma-Aldrich. The construct TRCN0000056554, which target sequence is 5′GCAGGATTGTT AGCAAAGAAA3′, was inserted in a pLKO.1-puro vector (Mission®, Sigma-Aldrich) following the manufacturer's instructions. Prior to transfection, the vector was linearized using the restriction enzyme *Sca*I (Fermentas-Thermo Scientific). SH-SY5Y cells were transfected with the linearized vector using Lipofectamine 2000 (Life Technologies, Inc., Gaithersburg, MD). Stable transfectants were selected in the presence of 1 μg/mL puromycin. Single clones were isolated by limiting dilution, transferred into 12-well plates, expanded, and selected by IRP1 expression, analyzing both protein levels and IRE-binding activity.

### 2.8. Determination of reduced and oxidized cysteines

The determination of reduced and oxidized cysteines was performed according to Horowitz et al. [34]. This technique is based in the labeling of reduced cysteines with fluorophore-tagged maleimides (Invitrogen–Thermo Fisher Scientific). Briefly, paraformaldehyde-fixed permeabilized SH-SY5Y cells were reacted with Alexa 488-tagged maleimide in order to label cysteines' SH groups. After washing, oxidized (S-S) cysteines were reduced with 5 mM tris(2-carboxyethyl) phosphine, followed by reaction with Alexa 568-tagged maleimide. The 488/568 fluorescence ratio was determined in a Zeiss LSM 510 Meta confocal laser scanning microscope (Carl Zeiss, Gottingen, Germany), and the values were translated into a pseudo-color scale by using the ImageJ image processing software (National Institutes of Health, USA).

### 2.9. 4-HNE immunofluorescence

Cells grown in cover slips were fixed with 4% paraformaldehyde, 4% sucrose in saline, permeabilized with 0.2% Triton-X-100 in PBS, incubated overnight at 4 °C with anti-HNE antibody (1:200) followed by incubation with Alexa-546-conjugated goat anti-rabbit IgG. The labeled cells were observed in a Zeiss LSM 510 Meta confocal laser-scanning microscope.

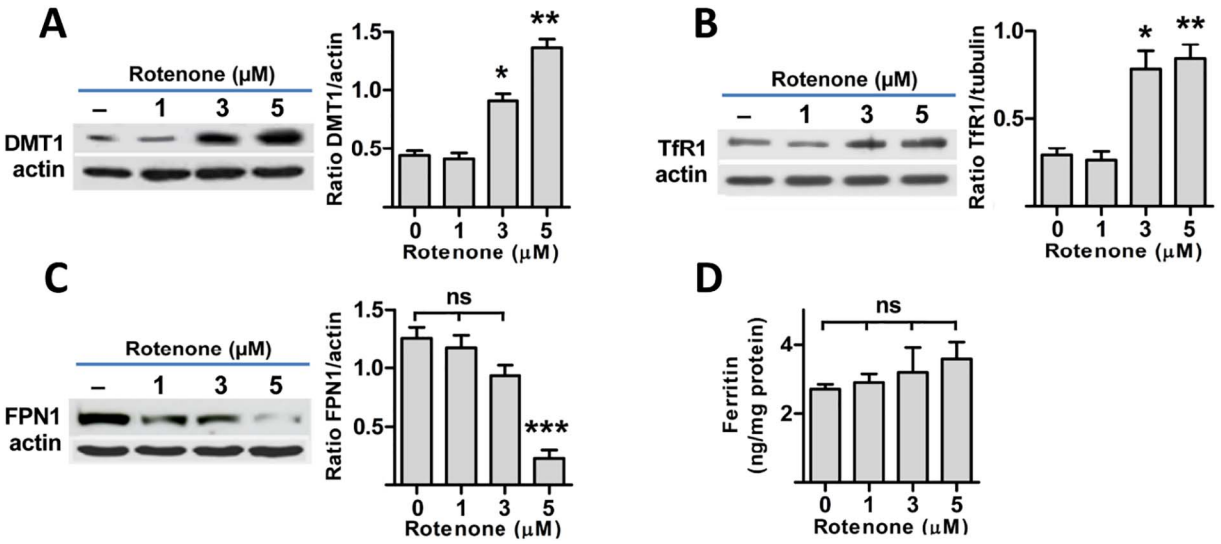


**Fig. 1.** Effects of complex I inhibition on iron homeostasis proteins. Protein extracts from cells treated for 24 h with 1, 3 or 5 μM rotenone were resolved by SDS-PAGE and changes in proteins of iron homeostasis, (A) DMT1, (B) TfR1 and (C) FPN1, were detected by Western blot. Actin or tubulin were used as load controls. Right-hand panels show quantification of band density. Values represent the mean ± SEM from 4 to 6 independent determinations. (D) Changes in ferritin protein levels estimated by ELISA. Significance was determined by one-way ANOVA followed by Tukey post-hoc tests. * $P < 0.05$; ** $P < 0.01$; *** $P < 0.001$ compared to control (no rotenone); ns, not significant change.

### 2.10. Data analysis

The experiments were repeated at least three times. The Shapiro-Wilk test was used in order to evaluate for normal distribution of replicates. One-way ANOVA was used to test the differences in mean values and Turkey's post-hoc test was used for comparisons (InStat, GraphPad Prism, San Diego, CA).

## 3. Results

### 3.1. Complex I inhibition modifies the expression of iron homeostasis proteins

Following on the observation that inhibition of mitochondrial complex I results in augmented IRP1 binding activity [20,21] (Supplementary Fig. 1), we tested if inhibition of complex I resulted in changes of the iron homeostasis proteins, which expression is translationally regulated by the IRE/IRP system. Rotenone treatment resulted in significantly increased levels of DMT1 (Fig. 1A) and TfR1 (Fig. 1B) and in decreased levels of FPN1 (Fig. 1C). The protein levels of ferritin, another IRP-regulated protein, did not show a significant increment upon rotenone treatment (Fig. 1D). The lack of a significant change in ferritin levels may be due to a compensatory transcriptional regulation process, since an oxidative stress response gene whose transcription is upregulated also codes ferritin by oxidative stress [35,36].

### 3.2. Inhibition of complex I increases iron uptake and the cytoplasmic labile iron pool

We then tested if the observed changes in iron transport proteins resulted in increased iron uptake and increased levels of redox-active iron in complex I-inhibited cells. $^{55}$Fe uptake experiments showed that rotenone-treated cells had increased iron uptake activity (Fig. 2A). In accordance with increased iron uptake, an increment in the cytoplasmic labile iron pool was also observed (Fig. 2B).

### 3.3. Inhibition of complex I induces iron-dependent oxidative damage

Because the cytoplasmic labile iron pool is redox-active [37,38], it was of interest to test whether increases in this pool resulted in oxidative damage. Rotenone treatment resulted in a marked increase in the formation of protein-HNE adducts (Fig. 3). 4-HNE is a very reactive lipid peroxidation product derived mostly from arachidonic and linoleic acid peroxidation. In proteins, 4-HNE forms adducts with the ε-amino group of lysines, the sulfhydryl group of cysteines and the imidazole group of histidines [39,40]. Thus, the formation of 4-HNE-protein adducts is a reflection of both lipid peroxidation and oxidative protein modification. Importantly, the increase in the oxidative modification was abolished by co-treatment with the iron chelators DFO, M30 and Q1 (Fig. 3C). Overall, the above results are consistent with the notion that inhibition of complex I results in increased redox-active iron, increased intracellular oxidative tone and increased oxidative damage. It is of note that rotenone treatment significantly decreased cell size, while co-treatment with rotenone and the iron chelators DFO, M30 or Q1 abolished this cell size decrease (Supplementary Fig. 2).

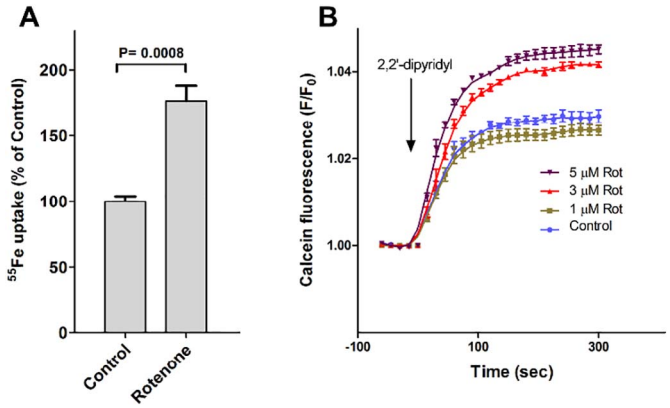


**Fig. 2.** Inhibition of complex I results in increased intracellular iron levels. (A) Cells were treated for 24 h with the complex I inhibitor rotenone (3 μM) after which $^{55}$Fe uptake was performed as described in Material and methods. Values are the mean ± SEM of a representative experiment ($N = 4$) with conditions done in triplicates. $P$ value was determined by the Student $t$-test. (B) Labile iron pool determination in cells treated for 24 h with the stated concentrations of rotenone. Cells were treated for 24 h with none, 1, 3 or 5 μM rotenone. Cells were then loaded with calcein-AM for 15 min at 37 °C. After change of medium, calcein fluorescence was dequenched with the iron chelator 2,2′-dipyridyl. Calcein dequenching under these conditions is proportional to the level of the cytoplasmic labile iron pool. Values are mean ± SEM of a representative experiment ($N = 3$) with conditions done in pentaplicate.

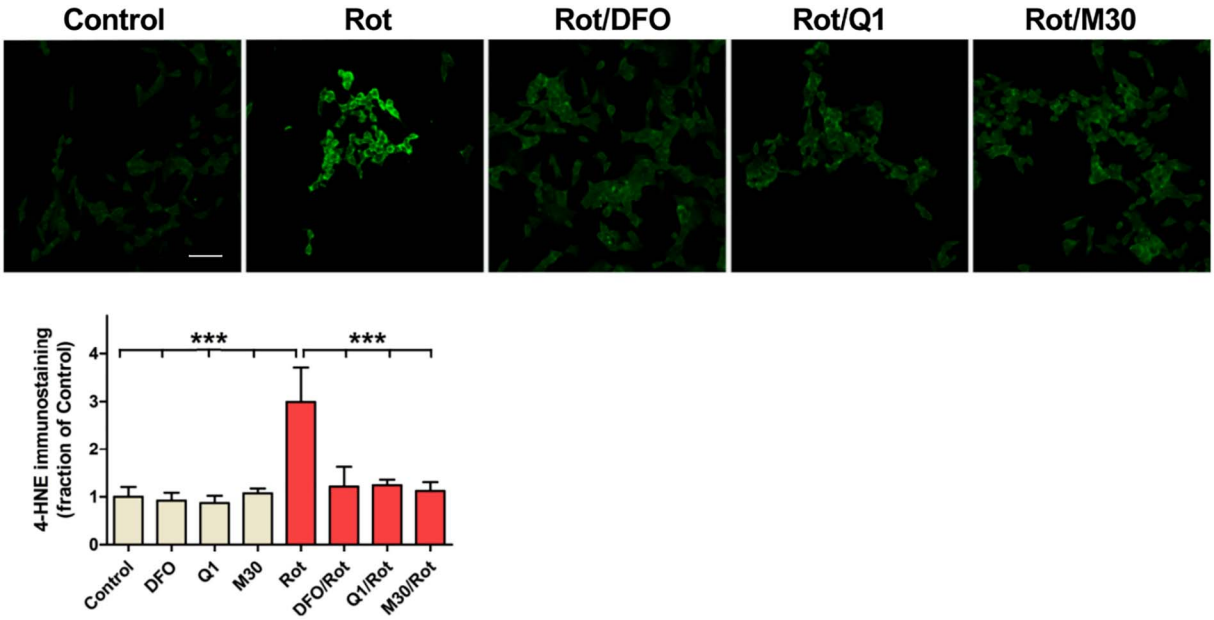


**Fig. 3.** Inhibition of complex I induces iron-mediated oxidative modifications. SH-SY5Y cells were treated for 24 h with or without 3 μM rotenone in the presence or absence of 5 μM DFO, 2.5 μM Q1 or 2.5 μM M30. The upper panel shows representative images of oxidative modifications assessed by immunodetection of 4-HNE adducts. Size bar: 50 μm. The lower panel shows quantification of 4-HNE immunofluorescence relative to Control (mean ± SEM) determined in 40–50 individual cells per experimental condition. *** $P < 0.0001$.

### 3.4. IRP1 knockdown

To evaluate the role of IRP1 in the oxidative phenotype observed after rotenone treatment, we used stable IRP1 knockdown cells in order to test their response to rotenone and oxidative challenges. From seven stable cell clones, cell clone 2.9 (from here on called shIRP1-2.9), which displayed 87% IRP1 protein knockdown (Fig. 4A) and decreased IRE binding activity (Fig. 4B) was selected for further experiments. In some of the experiments, clone 2.10 (here on called shIRP1-2.10) that displayed 34% IRP1 knockdown was also used.

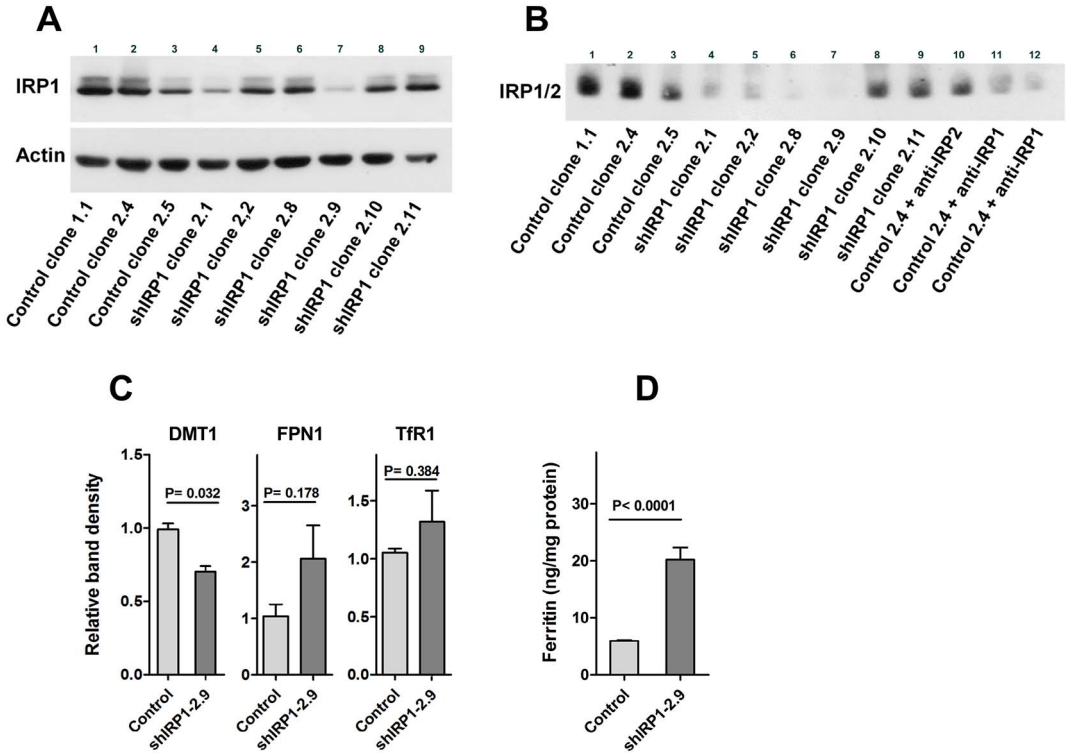


**Fig. 4.** IRP1 knockdown cells have increased ferritin levels. (A) SH-SY5Y cells were treated with IRP1 shRNA and stable clones were selected as described in Material and methods. IRP1 protein was detected by Western blot. Lines 1–3: cell clones 1.1, 2.4 and 2.5 from cells transfected with the empty vector. Lines 4–9: clones 2.1, 2.2, 2.8, 2.9, 2.10 and 2.11 from cells transfected with IRP1 shRNA. (B) IRE binding activity of clones determined by EMSA. Lines 1–3: clones 1.1, 2.4 and 2.5 from cells transfected with the empty vector. Lines 4–9: clones 2.1, 2.2, 2.8, 2.9, 2.10 and 2.11 from cells transfected with shRNA for IRP1. Line 10: extract from clone 2.4 treated with anti-IRP2 antibody before electrophoretic separation. Lines 11 and 12: extract from clone 2.4 treated with dilutions 1:500 and 1:250 of anti-IRP1 antibody before electrophoretic separation. (C) Extracts from control and clone 2.9 cells were evaluated for DMT1, FPN1, and TfR1 by Western blot. Shown is mean ± SEM ($N = 3$) of band density relative to the housekeeping protein actin. (D) Ferritin content evaluated by ELISA. Values are mean ± SEM of a representative experiment ($N = 5$) with conditions done in pentaplicate.

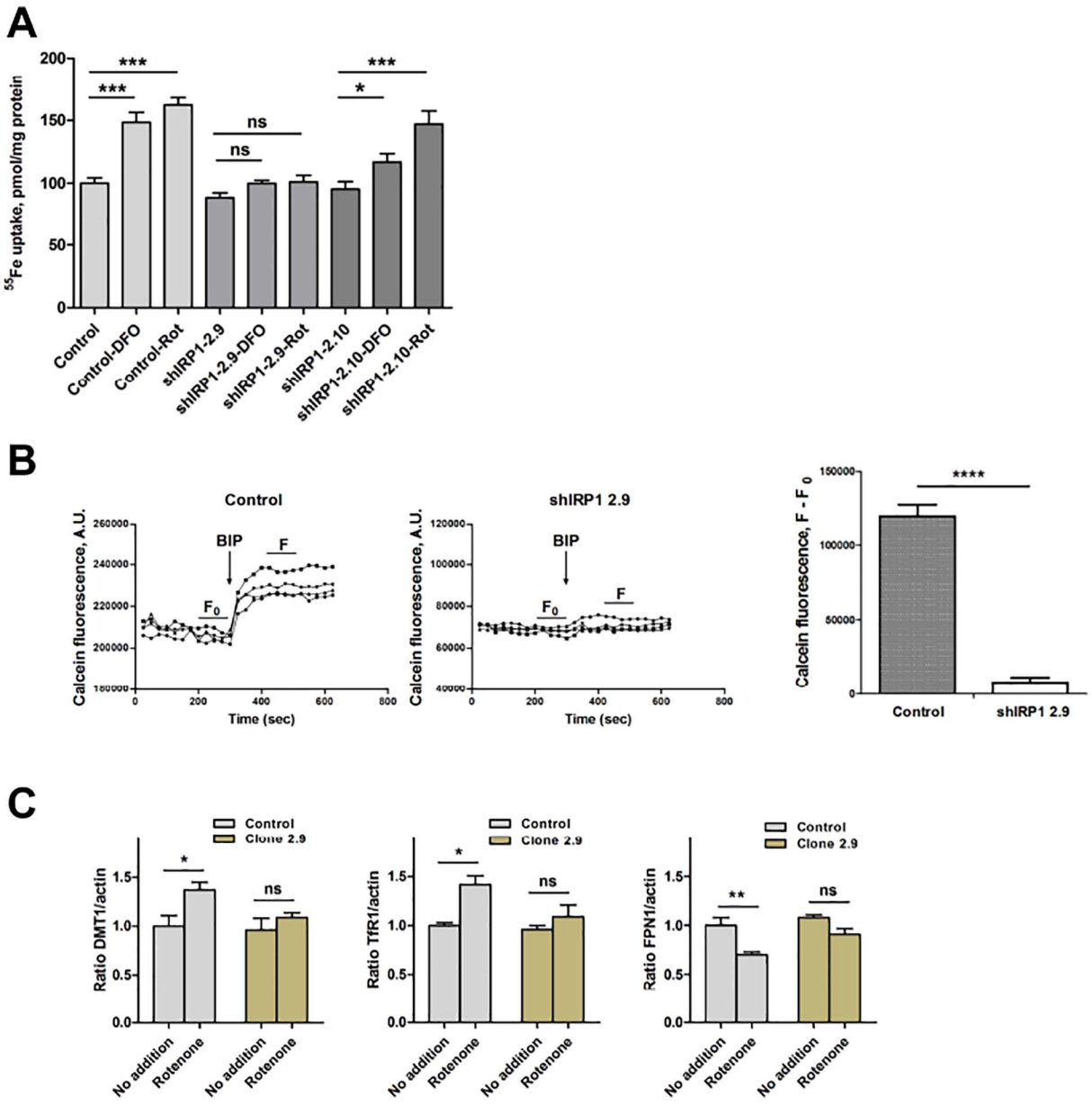


**Fig. 5.** $^{55}$Fe uptake by IRP1 knockdown cells. (A) Control or shIRP1-2.9 cells were incubated for 24 h with or without 3 μM rotenone (Rot) or 5 μM desferoxamine (DFO). ShIRP1-2.10 cells, which show a lesser decrease in IRP1 expression, were used as an additional control. Cells were tested for $^{55}$Fe uptake as described in Material and methods. Shown is mean ± SEM of pooled data from 6 independent experiments, with experimental points done in triplicates. Significance was determined by one-way ANOVA followed by Tukey post-hoc test. * $P < 0.05$; *** $P < 0.001$; ns, not significant. (B) Detection of the labile iron pool by calcein dequenching in control cells (left-hand panel) and shIRP1-2.9 cells (middle panel). Shown are 4 traces from individual wells. Right-hand panel shows quantification of the change in fluorescence ($F/F_0$) upon addition of the iron chelator 2,2′-dipyridyl (BIP). $F_0$ values were determined as the mean of fluorescence values at times between 200 and 300 s. F values were determined as the mean of fluorescence values at times between 420 and 520 s. **** $P < 0.0001$ as determined by two-tailed unpaired *t*-test. (C) Control or shIRP1-2.9 cells were incubated for 24 h with or without 3 μM rotenone and the protein levels of DMT1, TfR1 and FPN1 were estimated by Western blot analysis. Values were normalized to the Control condition. They are expressed as the mean ± SEM from 6 (DMT1), 3 (TfR1) or 4 (FPN1) independent determinations. Significance was determined by one-way ANOVA followed by Tukey post-hoc test. * $P < 0.05$; ** $P < 0.01$ as compared to Control; ns, not significant.

ShIRP1-2.9 cells had a small but significant decrement in DMT1 expression, with non-significant changes in FPN1 and TfR1 as compared to control cells (Fig. 4C). Unexpectedly, a three-fold increase in ferritin expression was detected in shIRP1-2.9 cells (Fig. 4D).

### 3.5. $^{55}$Fe uptake by shIRP1-2.9 cells

We next studied iron uptake activity by IRP1 knockdown cells in response to rotenone treatment (Fig. 5). Treatment with the iron chelator DFO was used as a positive control. The shIRP1-2.10 cells, with a minor knockdown of IRP1, were used as a secondary positive control.

Control and shIRP1-2.10 cells responded to the iron depletion induced by DFO treatment by increasing their $^{55}$Fe uptake activity while shIRP1-2.9 did not. Rotenone treatment induced $^{55}$Fe uptake in control and shIRP1-2.10 cells, but not in shIRP1-2.9 cells. The response to rotenone was proportionally lower in shIRP1-2.9 cells than in control or shIRP1-2.10 cells, with a $^{55}$Fe uptake ratio in response to rotenone treatment (rotenone/no treatment) of 1.48, 1.13 and 1.23, for control, shIRP1-2.9 cells and shIRP1-2.10 cells, respectively. It was apparent that an important degree of IRP1 knockdown (87% for shIRP1-2.9 vs 34% for shIRP1-2-10) is required to ameliorate the iron uptake response generated by inhibition of mitochondrial complex I. Detection of the labile iron pool by calcein dequenching revealed a marked decrease in shIRP1-2.9 cells when compared to control cells (Fig. 5B). Control cells responded to a 3 μM-rotenone challenge by increasing protein levels of DMT1 and TfR1 and by decreasing the level of FPN1, whereas shIRP1-

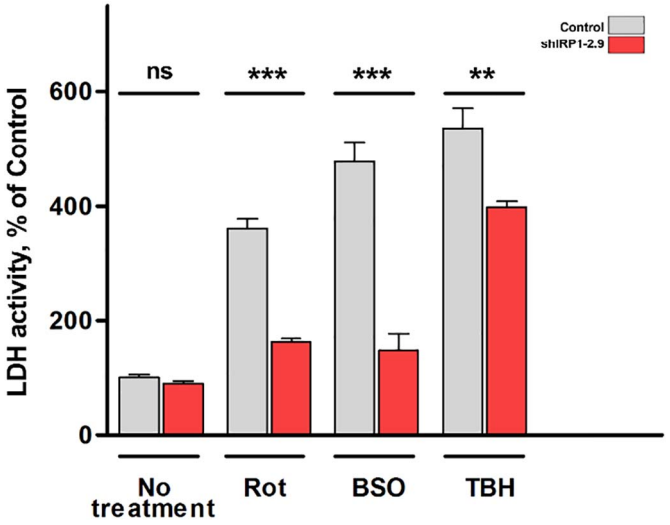


**Fig. 6.** Resistance to oxidant-induced cell death. Control or shIRP1-2.9 cells were incubated for 24 h either with 3 μM rotenone, 20 μM of the pro-oxidant *tert*-butylhydroperoxide (TBH) or with 50 μM of the glutathione synthesis inhibitor BSO, after which cell death was evaluated by LDH release into the culture medium. Values are expressed as the mean ± SEM with experimental points done in quintuplicates. Shown is a representative experiment ($N = 3$). Significance was determined by one-way ANOVA followed by Tukey post-hoc test. ** $P < 0.01$; *** $P < 0.001$; ns, not significant.

2.10 cells did not show significant changes in DMT1, TfR1 or FPN1 upon rotenone challenge (Fig. 5C).

### 3.6. IRP1 knockdown cells have increased resistance to oxidant-induced cell death and oxidative damage

ShIRP1-2.9 cells presented increased cell viability in response to rotenone as compared to control cells (Fig. 6). ShIRP1-2.9 cells also were more resistant than control cells to glutathione depletion induced by BSO and oxidant *tert*-butylhydroperoxide (TBH), although a larger LDH leak was observed upon TBH treatment. The resistance of IRP1 knockdown cells to oxidative death suggests that IRP1 is a mediator in the cell death induced by an increased oxidative tone.

### 3.7. IRP1 knockdown cells are resistant to oxidant-induced modifications

Inhibition of complex I results in increased ROS production, while an increased iron uptake may result in increased oxidative damage given the putative production of hydroxyl radical [41]. Thus, it was of interest to evaluate the response of IRP1 knockdown cells to rotenone and other oxidative stimuli. Rotenone treatment produced an increase of 4-HNE-protein adducts in control cells, an indication of increased lipid peroxidation. On the contrary, IRP1 knockdown cells exhibited a significant resistance to the formation of 4-HNE-protein adducts induced by rotenone (Fig. 7A and B).

To explore further the resistance of IRP1 knockdown cells to rotenone-induced oxidative stress we analyzed changes in the oxidized/reduced cysteine ratio in rotenone-treated cells. Rotenone dose-response studies showed that ShIRP1-2.9 cells had significant resistance to rotenone-induced cysteine oxidation at 1 and 3 μM rotenone but not at 5 μM rotenone (Fig. 7C and D). Similarly, shIRP1-2.9 cells showed significant resistance to the cysteine oxidation produced by iron overload (100 μM for 24 h, Fig. 7B). These results further support the idea that IRP1 mediates the oxidative damage derived from mitochondrial complex I inhibition by rotenone.

## 4. Discussion

Based upon previous findings showing that inhibition of complex I results in IRP1 activation [20,21], we examined here whether inhibition of mitochondrial complex I results in iron dyshomeostasis and oxidative damage, together with the putative participation of IRP1 in these phenomena.

We found that complex I inhibition resulted in increased expression of DMT1 and TfR1, and decreased expression of FPN1. These findings are reminiscent of reports showing both inhibition of complex I and increased expression of DMT1 in substantia nigra post-mortem tissue derived from PD patients [42,43], and in cell and animal models of the disease [44,45]. Arguably, both events, inhibition of complex I and increased expression of DMT1, could be linked by IRP1 activation.

We found decreased FPN1 levels upon complex I inhibition, a response that, together with increased DMT1 levels, should increase iron accumulation by cells. Decreased FPN1 protein levels were also reported as result of complex I inhibition by the dopamine metabolite aminochrome [22]. Similarly, 6-OHDA, a complex I inhibitor, induces FPN1 down-regulation and IRP1/IRP2 activation in primary ventral mesencephalic neurons [46]. Increased DMT1 expression and decreased FPN1 expression were accompanied by increased iron uptake and increased cytoplasmic labile iron pool. In addition, an increment in the oxidative tone and increased oxidative damage were detected upon complex I inhibition. Overall, the present results are consistent with a sequence of events in which inhibition of complex I results in increased iron uptake and increased iron retention by cells, with a corresponding increment in redox-active iron and oxidative damage.

The putative participation of IRP1 in this process was studied in IRP1 knockdown cells, which displayed a discrete decrement in DMT1 expression and non-significant changes in FPN1 and TfR1 levels when compared to control cells. These results suggest that in IRP1 knockdown cells translational regulation by IRP2 is sufficient to maintain DMT1, FPN1 and TfR1 close to control levels. Unexpectedly, a threefold increment in ferritin expression was detected in shIRP1-2.9 cells. At present, the causes for this increase are unknown, although IRP1 knock-out mice have been reported to have increased ferritin expression in brown fat and kidney, tissues that have high expression of IRP1 [47]. It is possible that in mice brown fat and kidney tissue, and in SH-SY5Y cells, ferritin mRNA translation is preferentially regulated by IRP1 in contrast to IRP2. Under this circumstance, IRP1 downregulation should result in increased ferritin translation.

IRP1 knockdown cells showed resistance to rotenone-induced cysteine oxidation and to the formation of 4-HNE adducts, together with a decreased loss of cell viability in response to rotenone, to the oxidant TBH and to inhibition of glutathione synthesis by BSO. This resistance to oxidative challenges again suggests that IRP1 participates in a process of cell death mediated by an increased oxidative tone. This view is consistent with the report that in neuron/glia mixed cultures, knockout of IRP2 or IRP1 increased neuronal resistance to $H_2O_2$ injury [48]. Rotenone treatment induced $^{55}Fe$ uptake in control cells but not in IRP1 knockdown cells. This result suggest that IRP1 mediates the increase in iron uptake in response to inhibition of mitochondrial complex I. Contrary to expectation, given the observed decrement in DMT1 protein in IRP1 knockdown cells, these cells had $^{55}Fe$ uptake similar to control. It is possible that the increased intracellular ferritin levels in IRP1 knockdown cells will drive iron uptake despite the decrease in DMT1 protein levels. Nonetheless, the increased ferritin expression may mediate the marked decrease in the cytoplasmic labile iron pool in IRP1 knockdown cells. Since the knockdown of HFn in shIRP1 cells increased the oxidative damage mediated by rotenone, most probably ferritin is the key mediator of the redox protective effect observed in IRP1 knockdown cells. This observation is in line with the observed increase of the labile iron pool and oxidant activity in K562 cells with repressed HFn synthesis [49].

In summary, our results show that in SH-SY5Y neuroblastoma cells: 1) mitochondrial complex I inhibition resulted in the change in expression of iron transporters and ferritin with a consequent increase in iron uptake and in the reactive iron pool; 2) mitochondrial complex I

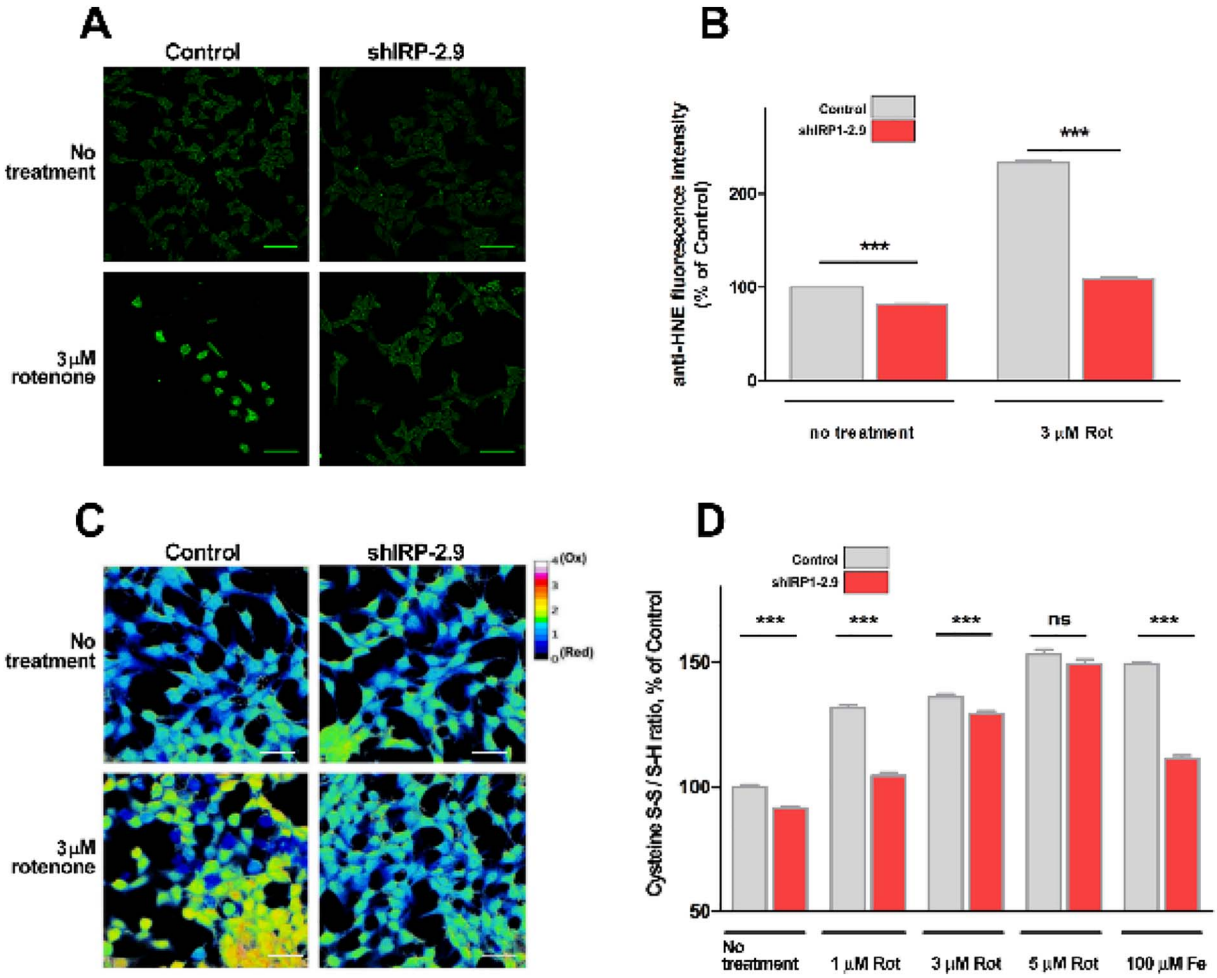


**Fig. 7.** IRP1 knockdown cells are resistant to rotenone-induced cysteine oxidation and protein modification. Control or shIRP1-2.9 cells were treated for 24 h with 3 μM rotenone after which cells were tested for oxidative damage and changes in their oxidative tone. (A) Representative image of 4-HNE immunostaining for the evaluation of oxidative damage. Size bars: 20 μm. (B) Quantification of 4-HNE immunostaining intensity upon treatment with rotenone for control and shIRP1-2.9 cells. Values are the mean ± SEM of 4-HNE immunofluorescence from 130 to 250 cells per experimental condition. (C) Oxidative tone evaluated by the amount of reduced and oxidized cysteine in proteins after treatment with rotenone. Maleimide-Alexa 488 (green) was used to detect reduced cysteines and maleimide-Alexa 568 (red) to detect oxidized cysteines. The ratio between red and green fluorescence was transformed (ImageJ program) into a thermal scale (right hand bar) in which a shift from blue to red to white implies a higher degree of oxidation. Size bars: 20 μm. (D) Quantification of the reduced/oxidized cysteine ratio upon treatment with 1, 3 or 5 μM rotenone. One hundred μM Fe-NTA was used as a positive control. The reduced/oxidized cysteine ratio of control cells without treatment was normalized to 1. Values are the mean ± SEM of fluorescence ratio from 85 to 168 cells per experimental condition. Significance was determined by one-way ANOVA followed by Tukey post-hoc test. *** $P < 0.001$; ns, not significant.

inhibition also resulted in an increased intracellular oxidative tone; 3) IRP1 knockdown largely suppressed the dysregulation of iron homeostasis induced by inhibition of complex I; 4) IRP1 knockdown also suppressed the increment in oxidative tone and oxidative damage induced by complex I inhibition; and 5) IRP1 knockdown provided cells with resistance against death promoted by oxidative stimuli, probably through increased ferritin expression and the consequent decrease in the labile iron pool. Taken together, these results are consistent with a mechanism by which inhibition of complex I results in increased IRP1 activity, iron accumulation and oxidative damage that may lead to cell death.

## Transparency document

The http://dx.doi.org/10.1016/j.bbadis.2017.05.015 associated with this article can be found, in the online version.

## Acknowledgements

Grant number 1130068 from the Fondo Nacional de Ciencia y Tecnología (FONDECYT) financed this work.

## Appendix A. Supplementary data

Supplementary data to this article can be found online at http://dx.doi.org/10.1016/j.bbadis.2017.05.015.

## References

[1] M.L. Wallander, E.A. Leibold, R.S. Eisenstein, Molecular control of vertebrate iron homeostasis by iron regulatory proteins, Biochim. Biophys. Acta 1763 (2006) 668–689.
[2] M.U. Muckenthaler, B. Galy, M.W. Hentze, Systemic iron homeostasis and the iron-responsive element/iron-regulatory protein (IRE/IRP) regulatory network, Annu. Rev. Nutr. 28 (2008) 197–213.
[3] B. Guo, J.D. Phillips, Y. Yu, E.A. Leibold, Iron regulates the intracellular degradation of iron regulatory protein 2 by the proteasome, J. Biol. Chem. 270 (1995) 21645–21651.
[4] J. Wang, K. Pantopoulos, Regulation of cellular iron metabolism, Biochem. J. 434 (2011) 365–381.
[5] D.L. Zhang, M.C. Ghosh, T.A. Rouault, The physiological functions of iron regulatory proteins in iron homeostasis — an update, Front. Pharmacol. 5 (2014) 124.
[6] C.P. Anderson, M. Shen, R.S. Eisenstein, E.A. Leibold, Mammalian iron metabolism and its control by iron regulatory proteins, Biochim. Biophys. Acta 1823 (2012) 1468–1483.
[7] E.S. Hanson, L.M. Foot, E.A. Leibold, Hypoxia post-translationally activates iron-regulatory protein 2, J. Biol. Chem. 274 (1999) 5047–5052.
[8] A.A. Salahudeen, J.W. Thompson, J.C. Ruiz, H.W. Ma, L.N. Kinch, Q. Li,

N.V. Grishin, R.K. Bruick, An E3 ligase possessing an iron-responsive hemerythrin domain is a regulator of iron homeostasis, Science (New York, N.Y.) 326 (2009) 722–726.
[9] A.A. Vashisht, K.B. Zumbrennen, X. Huang, D.N. Powers, A. Durazo, D. Sun, N. Bhaskaran, A. Persson, M. Uhlen, O. Sangfelt, C. Spruck, E.A. Leibold, J.A. Wohlschlegel, Control of iron homeostasis by an iron-regulated ubiquitin ligase, Science (New York, N.Y.) 326 (2009) 718–721.
[10] S.R. Smith, M.C. Ghosh, H. Ollivierre-Wilson, W. Hang Tong, T.A. Rouault, Complete loss of iron regulatory proteins 1 and 2 prevents viability of murine zygotes beyond the blastocyst stage of embryonic development, Blood Cells Mol. Dis. 36 (2006) 283–287.
[11] S.A. Schneider, K.P. Bhatia, Excess iron harms the brain: the syndromes of neurodegeneration with brain iron accumulation (NBIA), J. Neural Transm. (Vienna) 120 (2013) 695–703.
[12] M.A. Kurian, S.J. Hayflick, Pantothenate kinase-associated neurodegeneration (PKAN) and PLA2G6-associated neurodegeneration (PLAN): review of two major neurodegeneration with brain iron accumulation (NBIA) phenotypes, Int. Rev. Neurobiol. 110 (2013) 49–71.
[13] M. Gerlach, D. Ben-Shachar, P. Riederer, M.B. Youdim, Altered brain metabolism of iron as a cause of neurodegenerative diseases? J. Neurochem. 63 (1994) 793–807.
[14] H.H. Andersen, K.B. Johnsen, T. Moos, Iron deposits in the chronically inflamed central nervous system and contributes to neurodegeneration, Cell. Mol. Life Sci. 71 (2014) 1607–1622.
[15] M.C. Kruer, The neuropathology of neurodegeneration with brain iron accumulation, Int. Rev. Neurobiol. 110 (2013) 165–194.
[16] R.R. Crichton, D.T. Dexter, R.J. Ward, Brain iron metabolism and its perturbation in neurological diseases, J. Neural Transm. (Vienna) 118 (2011) 301–314.
[17] E.A. Martins, R.L. Robalinho, R. Meneghini, Oxidative stress induces activation of a cytosolic protein responsible for control of iron uptake, Arch. Biochem. Biophys. 316 (1995) 128–134.
[18] K. Pantopoulos, S. Mueller, A. Atzberger, W. Ansorge, W. Stremmel, M.W. Hentze, Differences in the regulation of iron regulatory protein-1 (IRP-1) by extra- and intracellular oxidative stress, J. Biol. Chem. 272 (1997) 9802–9808.
[19] C. Nuñez-Millacura, V. Tapia, P. Munoz, R.B. Maccioni, M.T. Nunez, An oxidative stress-mediated positive-feedback iron uptake loop in neuronal cells, J. Neurochem. 82 (2002) 240–248.
[20] N.P. Mena, A.L. Bulteau, J. Salazar, E.C. Hirsch, M.T. Núñez, Effect of mitochondrial complex I inhibition on Fe-S cluster protein activity, Biochem. Biophys. Res. Commun. 409 (2011) 241–246.
[21] D.W. Lee, D. Kaur, S.J. Chinta, S. Rajagopalan, J.K. Andersen, A disruption in iron-sulfur center biogenesis via inhibition of mitochondrial dithiol glutaredoxin 2 may contribute to mitochondrial and cellular iron dysregulation in mammalian glutathione-depleted dopaminergic cells: implications for Parkinson's disease, Antioxid. Redox Signal. 11 (2009) 2083–2094.
[22] P. Aguirre, P. Urrutia, V. Tapia, M. Villa, I. Paris, J. Segura-Aguilar, M.T. Nunez, The dopamine metabolite aminochrome inhibits mitochondrial complex I and modifies the expression of iron transporters DMT1 and FPN1, Biometals 25 (2012) 795–803.
[23] R.E. Heikkila, A. Hess, R.C. Duvoisin, Dopaminergic neurotoxicity of 1-methyl-4-phenyl-1,2,5,6-tetrahydropyridine in mice, Science (New York, N.Y.) 224 (1984) 1451–1453.
[24] H.M. Gao, J.S. Hong, W. Zhang, B. Liu, Synergistic dopaminergic neurotoxicity of the pesticide rotenone and inflammogen lipopolysaccharide: relevance to the etiology of Parkinson's disease, J. Neurosci. 23 (2003) 1228–1236.
[25] P. Aguirre, N. Mena, V. Tapia, M. Arredondo, M.T. Nunez, Iron homeostasis in neuronal cells: a role for IREG1, BMC Neurosci. 6 (2005) 3.
[26] P. Urrutia, P. Aguirre, A. Esparza, V. Tapia, N.P. Mena, M. Arredondo, C. Gonzalez-Billault, M.T. Nuñez, Inflammation alters the expression of DMT1, FPN1 and hepcidin, and it causes iron accumulation in central nervous system cells, J. Neurochem. 126 (2013) 541–549.
[27] R.S. Eisenstein, P.T. Tuazon, K.L. Schalinske, S.A. Anderson, J.A. Traugh, Iron-responsive element-binding protein. Phosphorylation by protein kinase C, J. Biol. Chem. 268 (1993) 27363–27370.
[28] N.P. Mena, O. García-Beltrán, F. Lourido, P.J. Urrutia, R. Mena, V. Castro-Castillo, B.K. Cassels, M.T. Núñez, The novel mitochondrial iron chelator 5-((methylamino) methyl)-8-hydroxyquinoline protects against mitochondrial-induced oxidative damage and neuronal death, Biochem. Biophys. Res. Commun. 463 (2015) 787–792.
[29] J.Y. Zhang, Y.N. Deng, M. Zhang, H. Su, Q.M. Qu, SIRT3 acts as a neuroprotective agent in rotenone-induced Parkinson cell model, Neurochem. Res. 41 (2016) 1761–1773.
[30] M. Jiang, Q. Yun, F. Shi, G. Niu, Y. Gao, S. Xie, S. Yu, Downregulation of miR-384-5p attenuates rotenone-induced neurotoxicity in dopaminergic SH-SY5Y cells through inhibiting endoplasmic reticulum stress, Am. J. Physiol. Cell Physiol. 310 (2016) C755–C763.
[31] F.K. Alkholifi, D.S. Albers, Attenuation of rotenone toxicity in SY5Y cells by taurine and *N*-acetyl cysteine alone or in combination, Brain Res. 1622 (2015) 409–413.
[32] M. Arredondo, A. Orellana, M.A. Garate, M.T. Nunez, Intracellular iron regulates iron absorption and IRP activity in intestinal epithelial (Caco-2) cells, Am. J. Phys. 273 (1997) G275–G280.
[33] S. Epsztejn, H. Glickstein, V. Picard, I.N. Slotki, W. Breuer, C. Beaumont, Z.I. Cabantchik, H-ferritin subunit overexpression in erythroid cells reduces the oxidative stress response and induces multidrug resistance properties, Blood 94 (1999) 3593–3603.
[34] M.P. Horowitz, C. Milanese, R. Di Maio, X. Hu, L.M. Montero, L.H. Sanders, V. Tapias, S. Sepe, W.A. van Cappellen, E.A. Burton, J.T. Greenamyre, P.G. Mastroberardino, Single-cell redox imaging demonstrates a distinctive response of dopaminergic neurons to oxidative insults, Antioxid. Redox Signal. 15 (2011) 855–871.
[35] Y. Tsuji, H. Ayaki, S.P. Whitman, C.S. Morrow, S.V. Torti, F.M. Torti, Coordinate transcriptional and translational regulation of ferritin in response to oxidative stress, Mol. Cell. Biol. 20 (2000) 5818–5827.
[36] K. Orino, L. Lehman, Y. Tsuji, H. Ayaki, S.V. Torti, F.M. Torti, Ferritin and the response to oxidative stress, Biochem. J. 357 (2001) 241–247.
[37] M. Kruszewski, Labile iron pool: the main determinant of cellular response to oxidative stress, Mutat. Res. 531 (2003) 81–92.
[38] O. Kakhlon, Z.I. Cabantchik, The labile iron pool: characterization, measurement, and participation in cellular processes (1), Free Radic. Biol. Med. 33 (2002) 1037–1046.
[39] H. Esterbauer, R.J. Schaur, H. Zollner, Chemistry and biochemistry of 4-hydroxynonenal, malonaldehyde and related aldehydes, Free Radic. Biol. Med. 11 (1991) 81–128.
[40] F. Khan, Moinuddin, A.R. Mir, S. Islam, K. Alam, A. Ali, Immunochemical studies on HNE-modified HSA: anti-HNE-HSA antibodies as a probe for HNE damaged albumin in SLE, Int. J. Biol. Macromol. 86 (2016) 145–154.
[41] M.T. Nuñez, P. Urrutia, N. Mena, P. Aguirre, V. Tapia, J. Salazar, Iron toxicity in neurodegeneration, Biometals 25 (2012) 761–776.
[42] J. Salazar, N. Mena, S. Hunot, A. Prigent, D. Alvarez-Fischer, M. Arredondo, C. Duyckaerts, V. Sazdovitch, L. Zhao, L.M. Garrick, M.T. Nunez, M.D. Garrick, R. Raisman-Vozari, E.C. Hirsch, Divalent metal transporter 1 (DMT1) contributes to neurodegeneration in animal models of Parkinson's disease, Proc. Natl. Acad. Sci. U. S. A. 105 (2008) 18578–18583.
[43] W.D. Parker, S.J. Boyson, J.K. Parks, Abnormalities of the electron transport chain in idiopathic Parkinson's disease, Ann. Neurol. 26 (1989) 719–723.
[44] H. Jiang, N. Song, H. Xu, S. Zhang, J. Wang, J. Xie, Up-regulation of divalent metal transporter 1 in 6-hydroxydopamine intoxication is IRE/IRP dependent, Cell Res. 20 (2010) 345–356.
[45] H.Y. Zhang, N. Song, H. Jiang, M.X. Bi, J.X. Xie, Brain-derived neurotrophic factor and glial cell line-derived neurotrophic factor inhibit ferrous iron influx via divalent metal transporter 1 and iron regulatory protein 1 regulation in ventral mesencephalic neurons, Biochim. Biophys. Acta 1843 (2014) 2967–2975.
[46] N. Song, J. Wang, H. Jiang, J. Xie, Ferroportin 1 but not hephaestin contributes to iron accumulation in a cell model of Parkinson's disease, Free Radic. Biol. Med. 48 (2010) 332–341.
[47] E.G. Meyron-Holtz, M.C. Ghosh, K. Iwai, T. LaVaute, X. Brazzolotto, U.V. Berger, W. Land, H. Ollivierre-Wilson, A. Grinberg, P. Love, T.A. Rouault, Genetic ablations of iron regulatory proteins 1 and 2 reveal why iron regulatory protein 2 dominates iron homeostasis, EMBO J. 23 (2004) 386–395.
[48] R.F. Regan, Z. Li, M. Chen, X. Zhang, J. Chen-Roetling, Iron regulatory proteins increase neuronal vulnerability to hydrogen peroxide, Biochem. Biophys. Res. Commun. 375 (2008) 6–10.
[49] O. Kakhlon, Y. Gruenbaum, Z.I. Cabantchik, Repression of the heavy ferritin chain increases the labile iron pool of human K562 cells, Biochem. J. 356 (2001) 311–316.